Mecánica Computacional Vol. XXI, pp. 2412–2430
S. R. Idelsohn, V. E. Sonzogni and A. Cardona (Eds.)
Santa Fe–Paraná, Argentina, October 2002

TOWARDS AN OPERATIONAL FORECASTING SYSTEM FOR THE RIO DE LA PLATA ESTUARY SURFACE ELEVATION AND CURRENTS

Claudia Simionato[(1)(2)], Walter Dragani[(2)(3)(4),] Mario Nuñez[(1)(2)] and Manfred Engel[(5)]

[(1)]Centro de Investigaciones del Mar y la Atmósfera (CIMA/CONICET-UBA), Argentina
[(2)]Departamento de Ciencias de la Atmósfera y los Océanos, FCEN, Universidad de Buenos Aires, Argentina
[(3)]Servicio de Hidrografía Naval (SHN), Argentina
[(4)]Consejo Nacional de Investigaciones Científicas y Técnicas (CONICET), Argentina
[(5)]Institut für Meereskunde (IfM), Universität Hamburg, Germany

Corresponding author address:
Ciudad Universitaria Pab. II Piso 2
1424, Ciudad Autónoma de Buenos Aires, Argentina
Phone: (54)(11)4787-2693 Fax: (54)(11)4788-3572
email: claudias@at.fcen.uba.ar, web page: http://www-cima.at.fcen.uba.ar

Key words: Numerical modeling, Río de la Plata, forecasting, variability, transports, currents, tides

Abstract. A set of three 3-D one-way nested models based on the baroclinic HamSOM (Hamburg Shelf Ocean Model) code for tidal propagation and storm surges from the Argentinean Continental Shelf to the Río de la Plata estuary has been developed. The set of models was constructed as a first step of the development of a warning and management system. In that sense they were built in a very realistic manner, representing an important advance with respect to previous works. In this paper some HamSOM/CIMA model hierarchy validation experiments are shown and discussed. Model results have been validated by using tidal gauge data and current meter observations. The model has shown an outstanding capability to reproduce the tidal propagation from the continental shelf to the Río de la Plata Estuary. A very good agreement between observations and model results is observed for both, harmonic constants and tidal currents. When wind stress and atmospheric pressure is included as meteorological forcing for our model, very good quality simulations are obtained. It indicates that our model already became an appropriate diagnostic tool for studies at the Río de la Plata. Results are very encouraging about the possibilities of the model to become a tool for forecasting and management.

1 INTRODUCTION

The Río de la Plata is one of the most important estuarine systems of the world and the most developed basin of eastern South America. It is exposed to frequent destructive floodings caused by the combination of tides and storm surges. Even though the Servicio de Hidrografía Naval of Argentina (SHN) maintains a warning system based on a statistical predictive method, a reliable operational numerical model for forecasting and coastal management of the Río de la Plata is not yet available. As the result of a cooperation, the construction of such a prediction tool is under development by CIMA and SHN, Argentina, and IfM, Germany. The objective of this co-operation effort is to develop 3-dimensional baroclinic models (that is, models that include the temperature and salinity distributions evolution) for the Argentinean Continental Shelf and, particularly, the Río de la Plata. The first goals of the development and application of numerical models in the area are:

- To understand and describe the physical systems and its behavior under the influence of the driving forces: atmospheric forcing (wind, air pressure, heat fluxes, etc.); tides and waves; fresh water discharge; interaction with the continental shelf/open ocean (salt water intrusion – maritime front, outer circulation system)
- To provide a tool for simulations and predictions of coastal zone with management purposes: storm surge warnings; pollution dispersion control; estimation of influences of construction measures (water ways, harbors, guide walls, etc.)

The baroclinic three-dimensional primitive equation Hamburg Shelf Ocean Model HamSOM is applied for this purpose. HamSOM, developed by the theoretical oceanography group of the Oceanographic Institute of the Hamburg University, has been adapted to the region and is been applied at CIMA as a set of three one way nested models. The largest domain lowest resolution Model A, covering the entire Argentinean Continental Shelf, provides boundary conditions to the intermediate resolution Model B, spanning the Río de la Plata estuary and the adjacent shelf. This model in turn, gives boundary conditions to a small-scale high-resolution model (C) of the Río de la Plata itself. This approach allows for a proper modeling of the estuary without the need of observational data to provide adequate boundary conditions to the models and, therefore, constitutes the base for an operational system.

HamSOM/CIMA model hierarchy might be applied in two ways:

- One is the “simulation mode” in which once appropriate boundary conditions are given to the model it reproduces the observed oceanic variables fields (surface elevation, currents, temperature, salinity, etc.) evolution under the changing driving forces.
- The second one is the “forecasting mode”. In this case forecasts for the driving forces (wind, atmospheric pressure and surface fluxes) are required. In this sense, the numerical atmospheric forecasting system already operational at CIMA will constitute a core part of the oceanic one.

Before considering the model as a reliable tool, a set of validation studies is being done. At a first approach to the goals, the model hierarchy has been applied to study the 3-D tide propagation and dynamics. Comparison to observations shows that HamSOM/CIMA model

hierarchy properly reproduces the observed tide regime, giving excellent estimations of the observed surface elevation values and tidal currents.

The next step in this investigation is the incorporation to the model of the wind and atmospheric pressure effect. Preliminary experiments were conducted in order to test the suitability of HamSOM/CIMA model to be used as a storm surge model system able to be applied with management purposes. Results have shown that the model provides excellent estimations of the observed wind driven sea surface elevation and currents.

In what follows, the HamSOM/CIMA model hierarchy will be introduced and some relevant results of the validation experiments will be shown and discussed.

2 DATA

The locations along the Argentinean and Uruguayan coast where sea level has been measured are shown Table 1. Geographical position of stations in the table can be found in Figure 1 by their associated indexes.

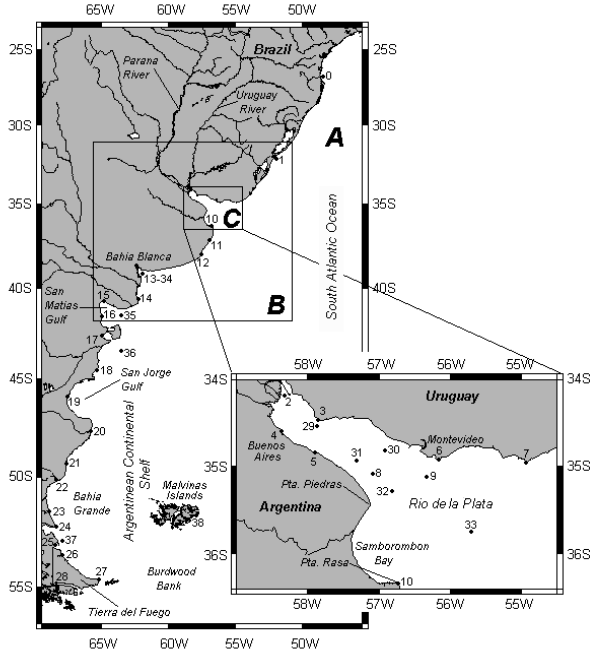

Figure 1. Map of the modeling area, showing the domain of every of the three models (A, B and C) and the location of the tidal gauge and current meter stations used for model validation. The names and exact location of the stations indicated by the indexes can be found in Tables 1 and 2.

These data were used to compute part of the harmonic constants presented in this paper. Tidal records were measured at standard tidal stations at sixteen locations, where sea levels were gathered by a basic tide gauge with a floater and counterweight inside a vertical tube[1]. The National Oceanic and Atmospheric Administration, USA (NOAA) and the SHN of Argentina installed three New Generation Water Level Measurement System (NGWLMS) at Mar del Plata, Punta Quilla and Ushuaia tidal stations. The NGWLMS tide gauge uses a dual system based in an acoustic and a pressure sensor. The acoustic sensor sends a shock of acoustic energy down a PVC sounding tube and measures the travel time for the reflected signals from a calibration reference point and from the water surface. The sensor controller performs the calculations to determine the distance to the water surface. The other system is based in a traditional pressure sensor to measure hydrostatic pressure of the water column at a fixed point and convert the pressure into a level.

Station (index)	Latitude (S)	Longitude (W)	Type of device	No. days
Martín García (2)	34° 11’	58° 15’	Floater	2920
Colonia (3)	34° 28’	57° 51’	Floater	730
Buenos Aires (4)	34° 34’	58° 23’	Floater	14965
La Plata (5)	34° 50’	57° 53’	Floater	365
Montevideo (6)	34° 55’	56° 13’	Floater	1460
Punta del Este (7)	34° 58’	54° 57’	Floater	365
Torre Oyarvide (8)	35° 06’	57° 08’	Floater	4745
Par Uno (9)	35° 10’	56° 19	Pressure sensor	330
San Clemente (10)	36° 21’	56° 23’	Floater	730
Pinamar (11)	37° 07’	56° 51’	Floater	1460
Mar del Plata (12)	38° 02’	57° 31’	NGWLMS	182
Puerto Belgrano (13)	38° 53’	62° 06’	Floater	301
San Blas (14)	40° 33’	62° 14’	Tide pole	38
San Antonio – E (15)	40° 48’	64° 52’	Tide pole	40
Punta Colorada (16)	41° 46’	65° 00’	Floater	271
Puerto Madryn (17)	42° 46’	65° 02’	Floater	13505
Santa Elena (18)	44° 31’	65° 22’	Tide pole	31
Cdro. Rivadavia (19)	45° 52’	67° 29’	Floater	1825
Puerto Deseado (20)	47° 45’	65° 55’	Floater	730
San Julián (21)	49° 15’	67° 40’	Tide pole	45
Punta Quilla (22)	50° 07’	68° 25’	NGWLMS	180
Río Gallegos (23)	51° 36’	69° 01’	Floater	729
Punta Vírgenes (24)	52° 30’	68° 28’	Tide pole	38
Ba. San Sebastian (25)	53° 10’	68° 30’	Tide pole	61
Río Grande (26)	53° 47’	67° 39’	Floater	180
Bahía Thetis (27)	54° 38’	65° 15’	Tide pole	139
Ushuaia (28)	54° 49’	68° 13’	NGWLMS	182

Table 1. Location of sea level gauge and duration of the series analyzed to obtain harmonic constants. Indexes in brackets refer locations to Figure 1.

Harmonic constants from eight places were calculated from tide pole measurements taken every 30 minutes or one hour. A pressure sensor (water level recorder Aanderaa model WRL-7) was installed in Par Uno at 8 m depth, 30 km south of Montevideo. This instrument was programmed with an interval sampling of 30 minutes. Finally, harmonic constants values from the Admiralty Tide Tables[2] were used to validate the model at the Brazilian locations Porto Bello and Río Grande (indexes 0 and 1 in Figure 1) and at the Malvinas Islands station Port Stanley (index 38 in Figure 1).

The positions of current meters whose data are employed in this paper can be found in Table 2 and identified in Figure 1 by their associated index.

Wind components at 10 m and atmospheric pressure data used in this paper come from NCEP-NCAR reanalysis. Full details of the NCEP-NCAR project and the dataset are given in Kalnay et al.[3] and discussions about its quality over the Southern Hemisphere can be found in Simmonds and Keay[4], among others.

Station (index)	Latitude (S)	Longitude (W)	Analyzed days	Depth (m)	Instrument Depth (m)	Instrument
PF-RDP (29)	34° 32’	57° 51’	71	5	3	rotor
CN-RDP (30)	34° 45’	56° 52’	66	10	5	rotor
QBO-RDP (31)	34° 49’	57° 19’	69	6	3	rotor
PPP-RDP (32)	35° 16’	56° 50’	60	6	1	rotor
B-RDP (33)	35° 52’	55° 37’	117	20	10	rotor
ER-BB (34)	39° 23’	61° 28’	36	15	3	rotor
B-GSM (35)	41° 37’	63° 40’	12	25	12	rotor
B-GN-3 (36)	43° 15’	63° 48’	269	81	27	acoustic
CN-TF (37)	52° 52’	68° 08’	10	38	18	rotor

Table 2. Location of current meters and duration of the series analyzed to obtain the tidal ellipses. Indexes in brackets refer locations to Figure 1.

3 MODEL DESCRIPTION

The model used for the numerical investigations is the HAMSOM (HAMburg Shelf Ocean Model), developed by Backhaus[5,6] at the Institut für Meereskunde (IfM) in Hamburg, Germany. Even though this model has been described at many publications[5,6,7,8,9,10,11], a brief description of the main equations solved and parameterization used is given in what follows. It is a three-dimensional multi-level (z coordinate) finite difference model, on the Arakawa C grid, based on the primitive equation set.

HamSOM is written in Cartesian coordinates. In order to account for the convergence of the meridians due to the spherecity of the Earth, all distances in the horizontal axis are computed as a function of latitude and the cell volume so considered is distorted for mass conservation purposes.

The code uses a two time level numerical scheme (present and future). To avoid instabilities, some terms of the equations are treated semi-implicitly (pressure gradient and

vertical diffusive stress) and the remaining ones explicitly. The Coriolis term is treated following the approach of Wais[12].

In order to derive and solve the discretized model equations first the momentum equations are vertically integrated in each layer; this way an expression for layer transports is found, which contains the unknown surface elevation (making the equation for the first layer to be non-linear) and vertical diffusive stresses. By vertically integrating again along the water column, the vertical diffusive stresses are canceled out and an expression for the vertically integrated transport is obtained. When this expression is substituted into the vertically integrated continuity equation (applied to a cell volume), an elliptic equation system for the increment of the water level is got. This last equation is solved by means of an iterative over relaxation technique, which is combined with a direct elimination algorithm in order to speed up the convergence. This way, after the parameterization of the diffusive and bottom stress terms, the equations for the layer velocities can be solved by direct elimination. Following the eddy viscosity analogy, the vertical diffusive stresses are parameterized as functions of the layer velocities; the vertical eddy mixing coefficients are updated using a mixing length expression[13] that accounts for turbulent effects in a local equilibrium way. The bottom stress is parameterized by means of a quadratic law in terms of the current velocity. For stability reasons, this term is treated semi-implicitly, being computed in the future time and in the present.

In order to avoid large jumps in the values of friction in areas where the depth of the bottom layer is very thin, bottom transport is computed in a layer of constant thickness (30 m) always that the total depth is higher than this value[8].

In our model hierarchy, the Río de la Plata estuary is reached through a set of three one-way nested models. The largest scale "Model A" covers an area spanning from 56.5º S to 23.5º S and from 69.5º W to 45.5º W (Figure 1). The horizontal resolution is of 20' in the zonal direction and 15' in the meridional one, what represents 27 Km approximately. Ten layers are employed in the vertical, whose bottoms are at 10, 20, 30, 60, 100, 200, 500, 1000, 3000 and 6000 m. This vertical discretization was selected to provide a good resolution in the upper layers and, therefore, solve properly the wind driven circulation. The minimum allowed depth is 5 m. Given the fact that ETOPO5 bathymetry data display unrealistic very shallow features over the Argentinean Continental Shelf, the topography has been built by combining this last data set with data provided by the Servicio de Hidrografía Naval of Argentina[14] for depths shallower than 200 m. The so obtained bathymetry is shown in the left panel of Figure 2, in which the most relevant features of the broad Argentinean shelf can be appreciated.

Model A provides boundary conditions to a higher resolution model of the Río de la Plata - adjacent Continental Shelf (Model B, Figure 1). This model spans the region between 42º S and 31.4º S, and 61.5º W and 51.5º W, with horizontal resolutions of 6.66' and 5', approximately 9 Km, respectively. In this case 13 vertical levels were used, with bottom at 4, 6, 10, 15, 20, 40, 60, 100, 200, 500, 1000, 3000 and 6000 m. Minimum allowed depth is 4 m in this case. The depth of the first layer is too high to properly resolve the shallow region of the Río de la Plata. Nevertheless, it has been set deep enough to properly solve the first layer at the south-westernmost areas of model domain, where the tidal amplitudes are known to be

large.

Finally, Model B provides boundary conditions to the highest resolution Model C (Figure 1) of the Río de la Plata. This covers the region between 36.5º S and 34.0º S and 59.0º W and 54.5º W, with horizontal resolutions of 1.8' and 1.5', approximately 3 Km, respectively. This model has 13 layers with bottom depths at 1, 2, 3, 4, 5, 6, 7, 10, 15, 25, 35, 45 and 55 m. The election of these levels allows for a good vertical resolution even at the very shallow areas of the upper Río de la Plata estuary.

High-resolution bathymetry data for models B and C were provided by the SHN and come from digitalization of charts[14,15,16,17,18]. The corresponding bottom topographies are shown in the right upper and lower panels of Figure 2 respectively. The large bathymetry gradients present in the region of interest are evident in the figure. Even the relatively small scale Model B has bottom depths that vary from centimeters at the upper estuary to 5500 meters at the outer shelf.

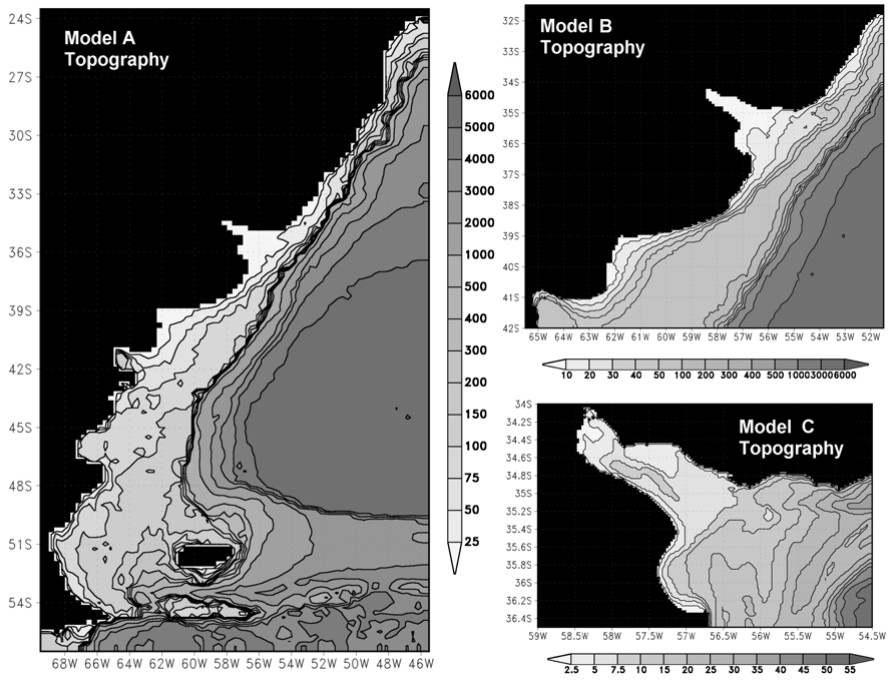

Figure 2. Bathymetry (isobaths in meters) for every of the three model domains. Note that the contour interval is neither regular nor the same for different figures.

4 RESULTS

4.1 Tidal amplitudes, phases and currents

At a first step in the validation, the model hierarchy has been applied to study the 3-D tide propagation and dynamics. In this case, model forcing was introduced by imposing tidal elevation at the open boundaries. The eight most important tidal constituents (M_2, S_2, N_2, K_2, O_1, P_1, K_1 and Q_1) were included in the simulation. In order to test the sensitivity of the solution to the boundary conditions, data derived from two different global models were used to force Model A. A bilinear interpolation routine was used to convert Zahel[19] and Ray et al.[20] one-degree resolution models outputs into amplitudes and phases at 20' X 15' resolution at the boundaries of Model A. Validation indicates that the solution forced with values coming from Zahel's model provides slightly better results. Nevertheless, it must be pointed out that even though a comparison between both global model outputs exhibits a slight difference in the amplitudes and phases at the southern part of the domain, our solutions do not result highly sensitive to it. For that reason, only the solution obtained with Zahel's boundary conditions will be shown along this paper.

The simulation time step for Model A was 5 minutes (300 seconds). With this relatively small time step, stability and absence of numerical damping and phase lags, which may occur at long time steps[21] are ensured.

In order to test model sensitivity to the horizontal eddy viscosity, different experiments for values of this parameter ranging from 100 to 600 $m^2\ s^{-1}$ were done. As long as the solutions do not exhibit sensitivity to the parameter the smaller value was selected for the solutions shown in this paper.

Model A was run for the equivalent to 12 months starting from rest. After approximately 10 days of simulation most of the transients due to the spin up of the model are dissipated. In order to ensure the stability of the solution the analysis was done by using only the last 8 months of the simulation with semi-hourly data. The analysis was done by means of a tidal analysis routine that follows the Foreman[22,23] approach to convert the simulated sea surface elevations into wave amplitudes and phases. Higher order harmonics like M_4 were also analyzed to study the non-linear sub modes generation at the shelf.

Once the amplitudes and phases were obtained for Model A, interpolation routines were used to get boundary conditions for Model B. Results do not exhibit sensitivity to variations between 50 and 200 $m^2\ s^{-1}$ of the horizontal eddy viscosity. Therefore, a value of 50 $m^2\ s^{-1}$ was chosen for the parameter in this case. The time step was 5 minutes (300 seconds), small enough to ensure stability and absence of numerical problems.

Finally, amplitudes and phases obtained from Model B are used to force Model C. For this last high-resolution model horizontal eddy viscosity was set to 50 $m^2\ s^{-1}$; results, once more, do not show sensitivity to variations of this parameter. The time step in this case was of 2.5 minutes (150 seconds).

Models B and C were also run for the equivalent to 12 months and the analysis to derive the harmonic constants was developed using the last 8 months of the simulation.

Table 3 shows a comparison between observed and simulated M_2 amplitudes and phases at locations of Figure 1 for every of the three model domains. In general all of the simulations provided results which are very consistent with what is known about the tidal propagation in the area and the comparison to observed tidal amplitudes and phases at coastal and island location was encouraging.

As an example, the simulated M_2 amplitudes and phases obtained from the harmonic analysis of the sea surface elevations provided by the simulation at the model C domain are shown in the upper panels of Figure 3. Results are highly consistent with what is known about the tidal propagation in the region. The tidal dynamics in the interior part of the estuary have been described by Balay[24,25] and simulated by O'Connor[26] and Vieira and Lanfredi[27]. These authors' results show that the range between the maximum and minimum of the tide is 0.8 m. The normal range of the tidal amplitude is around one meter on the Argentinean side, but only one third of this value on the Uruguayan side. This is not only a result of the fact that the tide is higher at the south than at the north of the estuary mouth, but also of the Coriolis effect. The wave propagates as a free external gravity wave along the estuary, with a phase velocity of $\sqrt{gH}$ (where H is the water depth). It takes the wave approximately 12 hours to propagate from one extreme to the other one. As this period is almost similar to the period of the tide, it can co-exist two maximums or two minimums at the same time within the estuary. This last feature is very clear in the simulated phases plot (Figure 3, upper right panel).

Station (index)	Observed		Model A		Model B		Model C	
	Amp.	Phase	Amp.	Phase	Amp.	Phase	Amp.	Phase
Porto Belo (0)	0.22	156	0.19	154				
Rio Grande (1)	0.04	345	0.06	328	0.08	335		
Martín García (2)	0.19	350	-	-	-	-	0.29	11
Colonia (3)	0.15	287	-	-	0.09	275	0.15	289
Buenos Aires (4)	0.27	302	-	-	0.11	339	0.28	304
La Plata (5)	0.23	243	0.23	244	0.22	245	0.25	239
Montevideo (6)	0.14	119	0.13	121	0.14	144	0.15	115
Punta del Este (7)	0.06	347	0.08	350	0.09	344	0.08	346
Torre Oyarvide (8)	0.32	146	-	-	0.27	166	0.33	152
Par Uno (9)	0.18	103	0.17	103	0.15	114	0.19	101
San Clemente (10)	0.36	11	0.37	14	0.39	14	0.42	12
Pinamar (11)	0.32	306	0.35	327	0.34	327		
Mar del Plata (12)	0.36	304	0.35	315	0.36	318		
Puerto Belgrano (13)	1.09	234	0.28	28	1.04	240		
San Blas (14)	0.82	159	0.27	125	0.75	157		
San Antonio – E (15)	3.14	72	3.23	84	3.36	85		
Punta Colorada (16)	2.84	63	2.78	78				
Puerto Madryn (17)	1.89	320	1.77	328				
Santa Elena (18)	1.63	269	1.73	262				
Cdro. Rivadavia (19)	2.06	220	1.96	221				
Puerto Deseado (20)	1.79	139	1.71	138				
San Julián (21)	2.83	75	3.15	76				
Punta Quilla (22)	3.74	52	3.77	55				
Río Gallegos (23)	3.85	45	3.90	35				
Punta Vírgenes (24)	3.20	7	3.43	11				
Ba. San Sebastian (25)	3.29	352	3.04	359				
Río Grande (26)	2.62	333	2.58	340				
Bahía Thetis (27)	1.27	299	1.40	300				
Ushuaia (28)	0.56	239	0.59	233				
Puerto Stanley (38)	0.43	277	0.44	281				
FS1 (39)	0.36	281	0.36	283				

Table 3. Observed and simulated M_2 harmonic amplitudes and phases for every of the three models. "–" sign is used for locations that are not solved because of model resolution.

The progression of the wave, northward and with the coast to the left, and the decay of the amplitude offshore are consistent with a response of Kelvin waves to the forcing at the shelf. The dynamics of the tides in terms of Kelvin waves is described by Gill[28] and discussed for the particular case of the Río de la Plata by O'Connor[26]. The Rossby radius of deformation is a scale of the decay offshore of the amplitude; taking as a representative depth of the estuary H=10 m, it results $\sqrt{gH}/|f| = 115Km$, which is narrower than the size of the estuary on its upper and medium parts. This fact, added to the importance of the dissipation in shallow waters ensures that there would not be an amphidromic system inside the estuary.

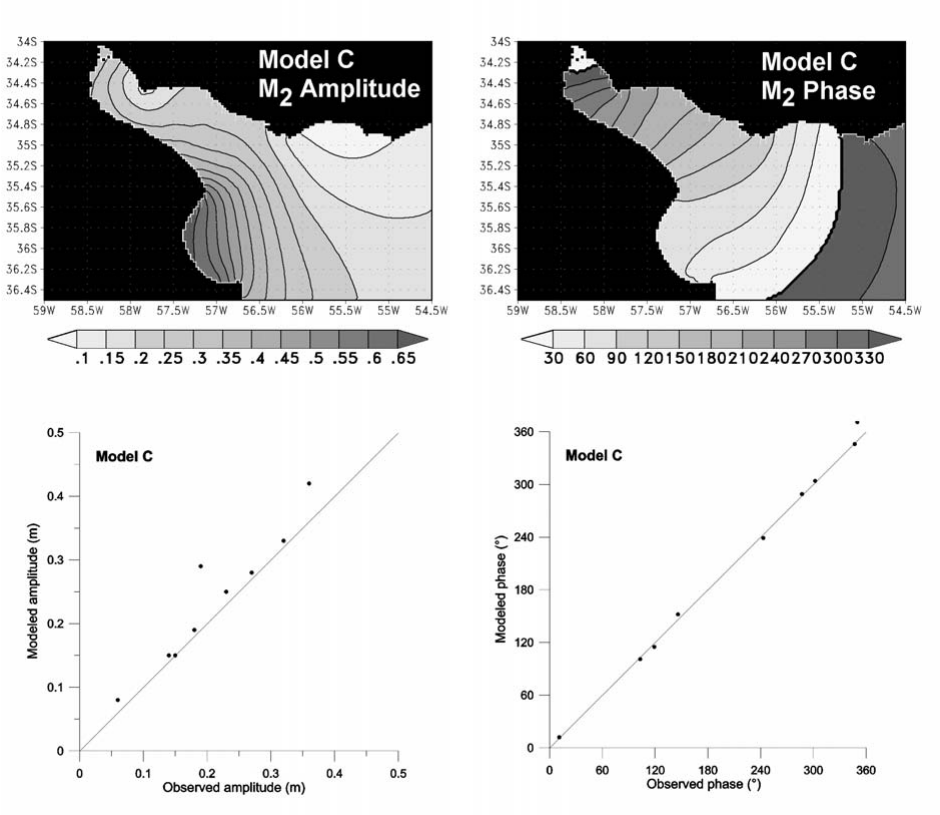

Figure 3. Upper panels: Corange (amplitudes in meters) and cotidal (phases in degrees) maps of the M_2 constituent from Model C. Lower panels: Scatter plots of modeled vs. observed amplitudes and phases for Model A simulation; the full line indicates the perfect fit.

All of these features are well described by Model C simulation, which displays a very good agreement with observations. Table 3 shows a comparison between observed and simulated amplitudes and phases at locations of Figure 1 for every of the three model domains. The errors of the amplitudes are of the order of a few centimeters and of the phase lags lower than 10 minutes excepting Oyarvide, where it is of around 13 minutes. The model only fails in reproducing the observed values at Martín García, a location on an island at mouth of the Uruguay River. The scatter plots of M_2 modeled vs. observed amplitudes and phases for this simulation are shown in the lower panels of Figure 3. Here simulated phases follow closely observations, whereas the model seems to overestimate slightly the amplitudes. The correlation coefficients are 0.99 for the phase and 0.91 for the amplitude including Martín García in the computation. Similarly encouraging results were obtained for all of the other tidal constituents.

In order to provide an idea of the effect of the small differences between the observed and simulated amplitudes and phases on the tidal forecast, Figure 4 displays a comparison between a forecast done with model C and the corresponding tidal table values at the San Clemente del Tuyú. The upper panel shows the instantaneous sea surface elevation anomaly produced by model C for October, 11, 1987 at 01:00z, meanwhile the lower panel displays the comparison between the modeled and observed values for this and the four previous days. A red star in the upper panel indicates the position of the station San Clemente del Tuyú. This last figure permits to appreciate that the model is able to forecast the tide with high accuracy.

In order to validate the tidal currents resulting from the simulations, M_2 HamSOM-generated tidal ellipses were compared with direct measurements at the locations 29 to 37 of Figure 1, whose characteristics are given in Table 2. Five of these observations correspond to the Río de la Plata estuary and the other four to locations on the continental shelf. Simulated velocities were interpolated to the current meter depth, which does not usually coincide exactly with model layer depth, and analyzed through a harmonic analysis routine in order to be compared with measured ellipses. Results show a general agreement between modeled and observed currents in both, speed and phase. Observations indicate speeds of almost 1 m s^{-1} at B-GSM and CN-TF (Table 2) that are properly reproduced by the simulations. In stations ER-BB and B-GN phase is satisfactory reproduced, even though the model tends to slightly overestimate the speed in the first of these stations.

Some M_2 observed and modeled tidal ellipses for the Río de la Plata estuary are displayed in Figure 5. It is observed that Model C tends to overestimate the zonal velocity component, meanwhile it reproduces well the meridional one and the phase.

Modeled tidal ellipses derived from the highest resolution Model C are displayed in Figure 6. Maximum speeds are obtained at the northernmost and southernmost tips of the Samborombón Bay, Punta Piedras and Punta Rasa, while in the interior of the Bay values are much smaller. This last region displays a rotational feature, but at the upper and central estuary the currents tend to be more unidirectional.

4.2 Preliminary experiments of wind driven surface elevation (surge) and currents

In order to evaluate the capability of HamSOM/CIMA model to reproduce the wind driven sea surface elevation (usually called surge) and currents, long period (several months) simulations in which the wind stress and atmospheric pressure effects were applied at the ocean surface, are being done for all those periods when currents direct observation for comparison are available.

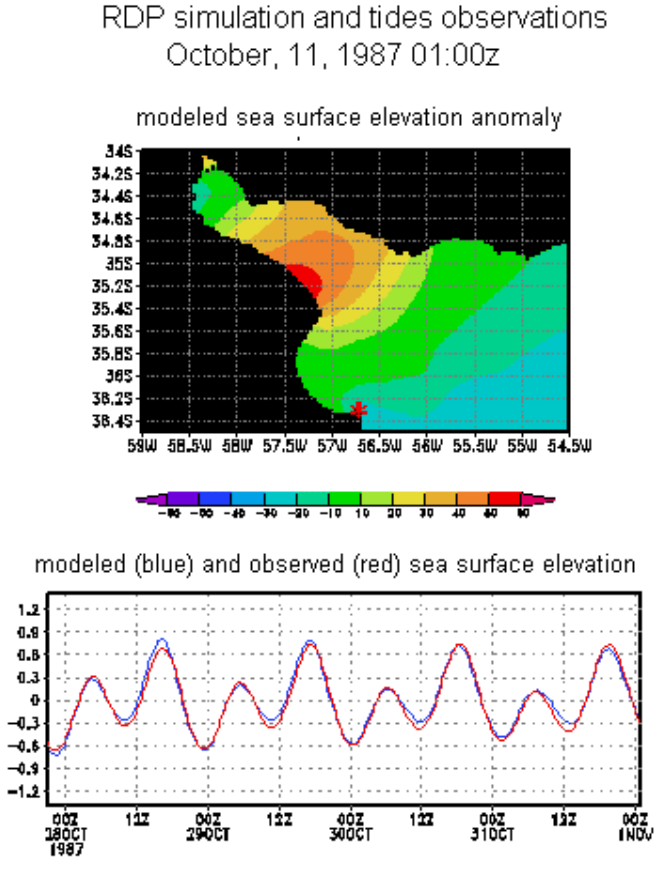

Figure 4: modeled and observed sea surface elevation due to tides at San Clemente del Tuyú (red star on the upper panel). The upper panel shows instantaneous sea surface elevation anomaly produced by model C for October, 11, 1987 at 01:00z, meanwhile the lower panel displays a comparison between the modeled and observed values.

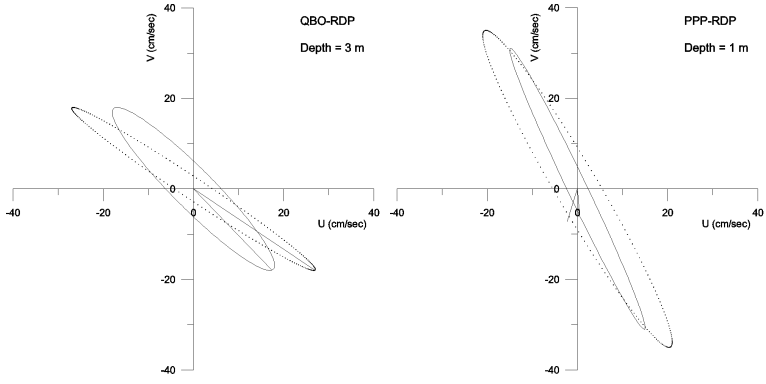

Figure 5. Comparison of measured (solid line) and computed (dotted line) M_2 tidal ellipses at different locations at the Río de la Plata estuary. The depth of the model layer at which the instrument was located is indicated.

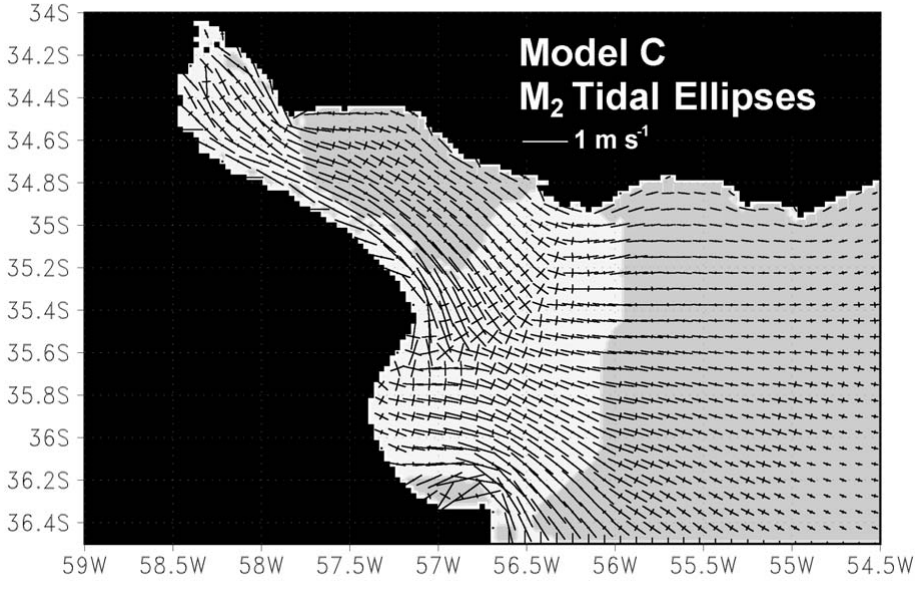

Figure 6. M2 tidal current ellipses derived from Model C. Shaded zones indicate counterclockwise rotation of the ellipses.

Given that model C area is too small to properly reproduce the surge, simulations were done by nesting this last model to model B. This way, at every time step, model B provides sea surface elevation boundary values to model C. The need of using model B for these kind of simulations requires the availability of large-scale good quality atmospheric data for forcing. Because most of the model B domain is oceanic, the few station data available on land are nor adequate to properly describe the wind pattern and its variability on that area. For that reason it was decided to force the oceanic model with data coming from an atmospheric operational model. Even though a very successful atmospheric forecast operational model (LAHM) is being run at CIMA, all the current-meter data available for doing these tests is previous to the moment when that model became operational. For that reason, the atmospheric data used in the simulations shown here come from the NCEP reanalysis project described in section 2. The main limitation of these reanalysis is its low resolution, of only 2.5º in latitude and longitude. Given that this is an on going work, only some preliminary results will be shown in what follows.

The results of a simulation performed for July, 1996 are shown in Figure 7. In the upper left panel, the sea surface elevation anomaly field for Jul., 7, 1996 at 10:00z can be observed, meanwhile the upper right panel displays the wind stress observed for that date and time. The lower panel shows a comparison between the modeled (blue) and observed (red) sea surface elevation for that day and hour and the previous days at Palermo (Buenos Aires). This last location is indicated as a red star in the upper left panel. Even though this figure only permits to appreciate the results for a given wind condition, high quality results were obtained for all of the simulations. For this particular three months simulation correlation coefficient between the observed and simulated elevations was of 0.86.

Even though usually the currents are much more difficult to reproduce than the sea surface elevations, very good results were obtained for this variable as well. As an example, Figures 8 shows the results of a simulation performed for December, 1987. In the upper left panel, the surface currents field for Dec., 8, 1987 at 15:00z can be observed, meanwhile the upper right panel displays the wind stress observed for that date and time. The lower panels show a comparison between the modeled (blue) and observed (red) zonal and meridional velocity components (left and right panels respectively) for that day and hour and the previous days at Bahía Samborombón. This last location is indicated as a red star in the upper left panel. The general visual agreement between the observed and simulated currents is very good. The correlation coefficient for the overall 2-months run was of 0.83 for the zonal velocity component and 0.73 for the meridional one. Similar results were obtained in the other simulations done.

Taking into account the relatively poor resolution (2.5º) of the atmospheric information used for the simulations and the fact that they are not really observed data but the results of an analysis, it is expected that the simulation results could be very much improved if regional model products (as LAHM/CIMA) were used to force the oceanic model.

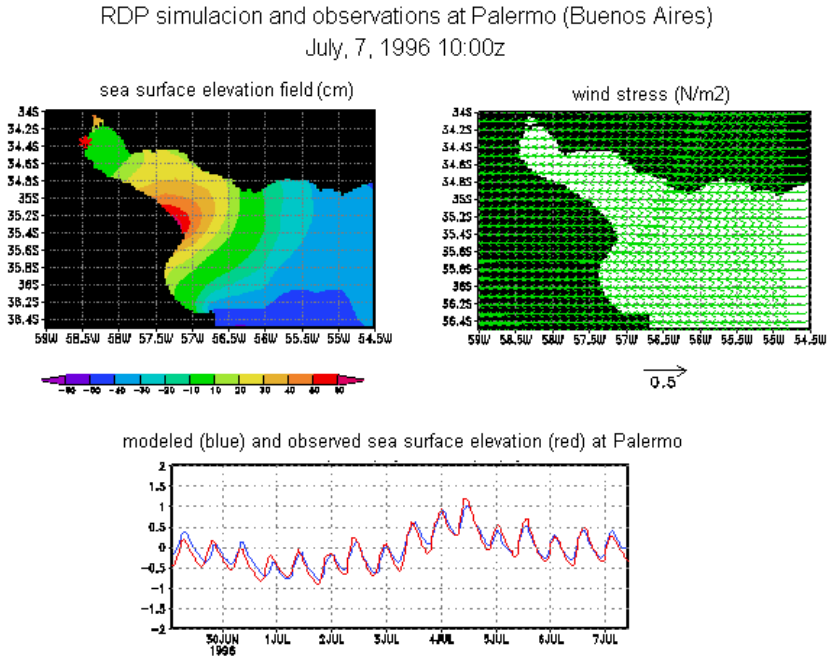

Figure 7: modeled and observed sea surface elevation at San Palermo (red star on the upper panel). The upper left panel shows instantaneous sea surface elevation anomaly produced by model C for July, 7, 1996 at 10:00z. The upper right panel displays the wind stress observed for that date. The lower panel displays a comparison between the modeled and observed values.

5 CONCLUSIONS

A set of three 3-D nested models based on HamSOM code for tidal propagation and storm surges from the Argentinean Continental Shelf to the Río de la Plata estuary has been developed. The set of models was constructed as a first step of the development of a warning and management system. In that sense they were built in a very realistic manner, representing an important advance with respect to previous works.

In this paper some HamSOM/CIMA model hierarchy validation experiments were shown and discussed. Model results have been validated by using tidal gauge data and current meter observations.

The model has shown an outstanding capability to reproduce the tidal propagation from the continental shelf to the Río de la Plata Estuary. A very good agreement between observations and model results is observed for both, harmonic constants and tidal currents. Therefore, we are confident that the validity of the data obtained by the simulations could be extended to

other areas where no tidal gauge and/or current meters are present and that the set of three one-way nested models can constitute the base of a useful management tool.

When the relatively poor resolution NCEP reanalysis wind stress and atmospheric pressure is used as meteorological forcing for our model, very good quality simulations are obtained. It indicates that our model already became an appropriate diagnostic tool for studies at the Río de la Plata.

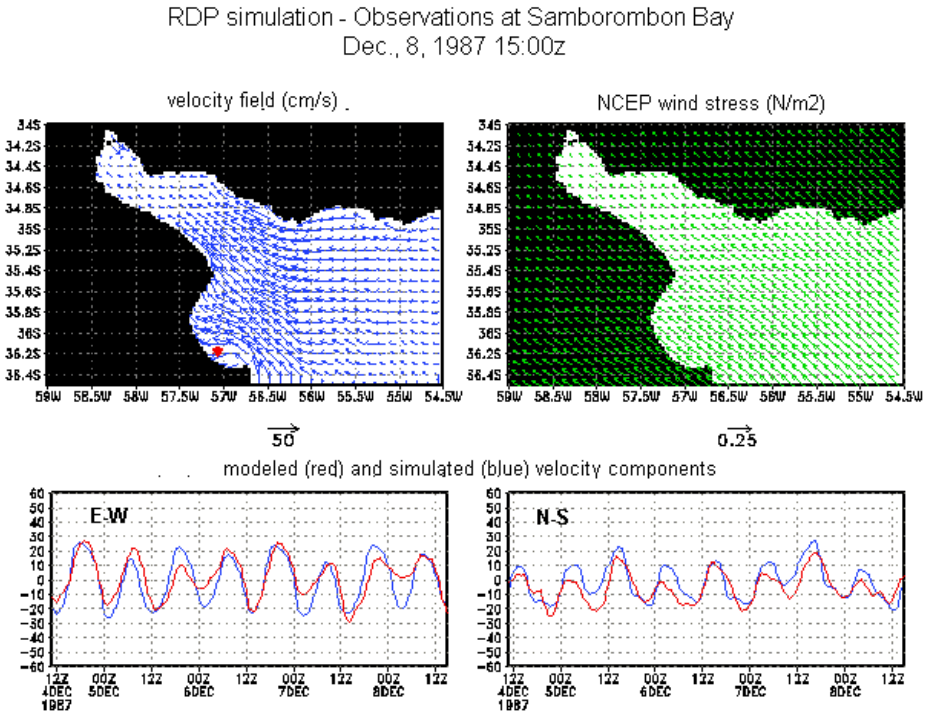

Figure 8: modeled and observed currents at Samborombón Bay (red star on the upper panel). The upper left panel shows instantaneous surface velocity field produced by model C for December, 8, 1987 at 15:00z. The upper right panel displays the wind stress observed for that date. The lower panel displays a comparison between the modeled and observed values.

Results are very encouraging about the possibilities of the model to become a tool for forecasting. Nevertheless, this will require the availability of higher resolution atmospheric model results and, if possible, direct wind and atmospheric pressure observations to validate those results. About atmospheric model forcing data, it is expected that the high resolution (60 Km) limited area model already operational at CIMA will provide enough accurate winds

and atmospheric pressure fields to force HamSOM.

At the moment being an improvement of the parameterization of momentum exchange between the ocean and the atmosphere in the oceanic model is being faced. It is being accomplished through the incorporation of a wind wave (WAVEWATCH 3) sub model. It is expected that this modification will highly improve the sea surface elevation forecast especially under extreme wind conditions.

The final step in the model construction will the addition of the temperature and salinity fields into the simulation, what requires the incorporation into the model of all of the ocean-atmosphere interaction processes. The availability of these variables has important consequences for applications to fisheries and nutrients, pollutants and sediment transports.

In the next future ADCP and drifters measurements will be collected in the context of the UNDP/GEF project "Environmental Protection of the Río de la Plata and its Maritime Front". These measurements will be very valuable to further validate our model results.

6 ACKNOWLEDGMENTS

This work was partially supported by SETCIP of Argentina and BMBF of Germany through the Co-operation Project AL/A98-UVII/15. Part of the research has been supported by UBA Grant X072 and BID-PICT 99-6215. Useful discussion with scientists of other institutions have resulted of cooperative work promoted by the UNDP/GEF project "Protección Ambiental del Río de La Plata y su Frente Marítimo" conducted by the Consortium CARP/CTMFM.

7 REFERENCES

[1] Unesco, 1985. Manual on sea level measurement and interpretation. Intergovernmental Oceanographic Commission, 83 pp.

[2] Hydrographers of the Navy, 2000. Admiralty Tide Tables, Europe (excluding United Kingdom and Ireland), Mediterranean Sea and Atlantic Ocean, vol. 2, NP 202-01-2001.

[3] Kalnay, E. and Coauthors, 1996. The NCEP/NCAR 40-Year reanalysis project. Bulletin of the American Meteorological Society, 77, 437-471.

[4] Simmonds, I and K. Keay, 2000. Mean Southern Hemisphere extra tropical cyclone behavior in the 40-year NCEP-NCAR Reanalysis. Journal of Climate, 13, 873-885.

[5] Backhaus, J. O., 1983. A semi-implicit scheme for the shallow water equations for application to shelf sea modelling. Continental Shelf Research, 2(4), 243-254.

[6] Backhaus, J. O, 1985. A three dimensional model for simulation of shelf sea dynamics. Deutsche Hydrographische Zeitschirft. 38(H.4), 164-187.

[7] Backhaus, J. O. and D. Hainbucher, 1985. A finite difference general circulation model for shelf sea and its applications to low frequency variability on the North European Shelf. In: Three dimensional model of marine and estuarine dynamics. J. C. Nihoul and B. M. Jamars, (Eds.). Elsevier Oceanographic Series. 45, Amsterdam, 221-244.

[8] Rodriguez, I. and E. Alvarez, 1991. Modelo tridimensional de Corrientes. Condiciones de aplicación a las costas españolas y análisis de resultados para el caso de un esquema de mallas anidadas. Clima Marítimo Report, 42, 65 pp.
[9] Rodriguez, I., E. Alvarez, E. Krohn and J. Backhaus, 1991. A mid-scale tidal analysis of waters around the north western corner of the Iberian Peninsula. Proceedings of a Computer Modelling in Ocean Engineering 91, Balkema, 568 pp.
[10] Stronach, J. A., J. Backhaus and T. S. Murty, 1993. An update on the numerical simulation of oceanographic processes in the waters between Vancouver Island and the mainland: the GF8 model. Oceanography and Marine Biology: An annual Review 31, 1-86.
[11] Alvarez Fanjul, E. A., B. Pérez Gómez and I. Rodríguez Sanchez-Arévalo, 1997. A description of the tides in the Eastern North Atlantic. Progress in Oceanography, 40, 217-244.
[12] Wais, R., 1985. On the relation of linear stability and the representation of Coriolis term in the numerical solution of the shallow water equations. PhD thesis. Hamburg University.
[13] Pohlmann, T., Untersuchung hydro- und thermo-dynamischer Prozesse in der Nordsee mit einem dreidimensionalen numerischen Modell. PhD. Thesis, Hamburg University, 1991.
[14] SHN, 1986, Mar Argentino, de Río de la Plata al Cabo de Hornos, Carta Náutica 50, 4th ed., Servicio de Hidrografia Naval, Armada Argentina.
[15] SHN, 1992, Acceso al Río de la Plata, Carta Náutica H1, 5th ed., Servicio de Hidrografia Naval, Armada Argentina.
[16] SHN, 1993, El Rincón, Golfo San Matías y Nuevo, Carta Náutica H2, 4th ed., Servicio de Hidrografia Naval, Armada Argentina.
[17] SHN, 1999a, Río de la Plata Medio y Superior, Carta Náutica H116, 4th ed., Servicio de Hidrografia Naval, Armada Argentina.
[18] SHN, 1999b, Río de la Plata Exterior, Carta Náutica H113, 2nd ed.,Servicio de Hidrografia Naval, Armada Argentina.
[19] Zahel, W., 1997. Ocean Tides, in Lecture Notes in Earth Sciences 66, Springer 1997: Tidal Phenomena, Helmut Wilhelm, Walter Zürn, Hans-Georg Wenzel (Eds.)
[20] Ray, R. D., B. V. Sanchez and D. E. Cartwright, 1994. Some extensions to the response method of tidal analysis applied to TOPEX/POSEIDON (abstract). EOS, Transactions of the American Geophysical Union, 75, 108 (srping Meeting Supplement).
[21] Kowalik, Z. and T. S. Murty, 1993. Numerical modeling of ocean dynamics. Advanced Series of Ocean Engineering. Vol. 5. World Scientific, 481pp.
[22] Foreman, M.G.G.,1977. Manual for tidal heights analysis and prediction. Pac. Mar. Sci. Rep. 77-10, Inst. of Ocean Sci., Patricia Bay, Sidney, B. C., Canadá, 97 pp.
[23] Foreman, M.G.G.,1978. Manual for tidal heights analysis and prediction. Pac. Mar. Sci. Rep. 78-6, Inst. of Ocean Sci., Patricia Bay, Sidney, B. C., Canadá, 70 pp.
[24] Balay, M. A., 1956. Determination of mean sea level of Argentine Sea. Influences of oscillations of the sea not caused by tides. International Hydrographic Review (Monaco),

33(2), 31-65.
[25] Balay, M.A., 1961. El Río de la Plata entre la atmósfera y el mar. Publi. H-621. Servicio de Hidrografía Naval. Armada Argentina. Buenos Aires. 153 pp.
[26] O'Connor, W. P., 1991. A numerical model of tides and storm surges in the Río de la Plata estuary". Continental Shelf Research, 11, 1491-1508.
[27] Vieira, A. and N. W. Lanfredi, 1996. A hydrodynamic model for the Río de la Plata. Journal of Coastal Research, 12(2), 430-446.
[28] Gill, A., 1982. Atmosphere-Ocean Dynamics. International Geophysics Series, Vol. 30. Academic Press Inc., San Diego, California, 662pp.